HEFAT2011
8th International Conference on Heat Transfer, Fluid Mechanics and Thermodynamics
11 – 13 July 2011
Pointe Aux Piments, Mauritius

HEAT AND WATER MANAGEMENT IN AN ALKALINE FUEL CELL

Ivan Verhaert [a,b,c] , Sebastian Verhelst [a], Griet Janssen[b], Grietus Mulder[c], Michel De Paepe[a]
a) Department of Flow, Heat and Combustion Mechanics,
Ghent University- UGent, Sint-Pietersnieuwstraat 41, 9000 Gent, Belgium
b) KHKempen,University College,
Kleinhoefstraat 4, 2440 Geel, Belgium
c) VITO, Flemish Institute for Technological Research,
Boeretang 200, 2400 Mol, Belgium
*Author for correspondence
E-mail: ivan.verhaert@khk.be

ABSTRACT

Alkaline fuel cells are low temperature fuel cells for which stationary applications, like cogeneration in buildings, are a promising market. To guarantee a long life, water and thermal management has to be controlled in a careful way. To understand the water, alkali and thermal flows, a two-dimensional model for an alkaline fuel cell module is developed using a control volume approach. Special attention is given to the physical flow of hydrogen, water and air in the system and the diffusion laws are used to gain insight in the water management. The model is validated on the prediction of the electrical performance and thermal behaviour. The positive impact of temperature on fuel cell performance is shown. New in this model is the inclusion of the water management, for which an extra validation is performed. The model shows that a minimum temperature has to be reached to maintain the electrolyte concentration. Increasing temperature for better performance without reducing the electrolyte concentration is possible with humidified hot air.

INTRODUCTION

Our future energy market will have to find solutions to stop our growing energy demand and to integrate as much renewable energy as feasible on the supply side. This will lead to an future energy market in which distributed generation will play a significant role [1]. At the demand side buildings are still responsible for a large part of energy use. In this prospect micro combined heat and power (micro-CHP) systems for building applications are getting more attention [2, 3].

Compared to other technologies fuel cell based systems have a high power to heat ratio even at small sizes, because they are modularly built. Therefore, fuel cell based micro-CHP have the potential to reduce gas emissions and primary energy use in residential dwellings or buildings with a relatively low heat de-mand [4, 5, 6]. Four prominent fuel cell technologies are suitable as micro - CHP for building applications: solid oxide fuel cells (SOFC), proton exchange membrane fuel cells (PEMFC), phosphoric acid fuel cells (PAFC) and alkaline fuel cells (AFC) [7].

Compared to the others the AFC hass the potential of a cheaper construction, as it can be produced by relatively standard materials and does not require precious metals [8, 9]. This led to renewed interest in AFC technology [5, 9]. Next to lifetime improvements and handling degradation, the biggest advancements and reduction in total environmental impact are to be expected in reducing catalyst loading and optimising the overall system [5].

To optimise the overall system of a more compact and more energy efficient AFC-based micro-CHP for buildings it is necessary to understand the complete heat and water management of an AFC. In earlier work a thermal model of an alkaline fuel cell was built in Aspen Custom Modeller [11]. The model combined prediction of electrical performance and thermal behaviour, but had no interest in water management. The objective of this study is to build a model which provides insight in the water management of the fuel cell and to study new control strategies for an AFC system.

NOMENCLATURE

Q	[W]	*heat*
T	[K]	Temperature
z	[cm]	1D distance over diffusion layer
P	[Pa]	Presure
R	[J/kg.K]	Universal gas constant
y	[-]	Molar fraction
N	[mol/(s.m²)]	Molar flux
D	[cm²/s]	Diffusion coefficient

Subscripts

w	Water / Water vapour
H	Hydrogen

MODEL DEVELOPMENT

General operation

An overview of the general operation of an AFC system is given in [12]. As shown in Figure 1 an AFC operates by introducing hydrogen at the anode and oxygen/air at the cathode.

- At the hydrogen inlet a gas mixture of water vapour and hydrogen enters the gas chamber of the fuel cell. The hydrogen diffuses out of the gas chamber into the working area of the anode.
- At the oxygen inlet CO2-free air or pure oxygen arrives in the gas chamber. The oxygen diffuses into the working area of the cathode to take part in the reaction.

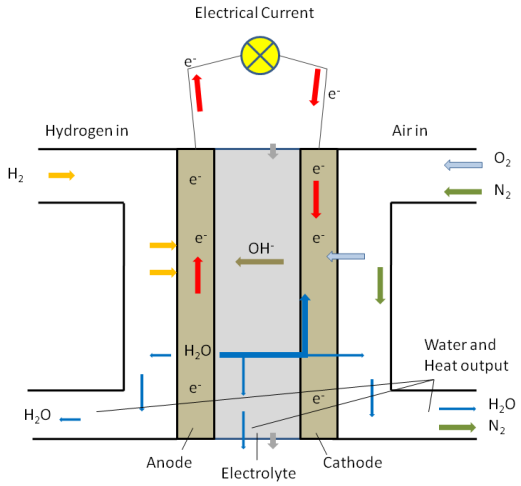

Figure 1 *Working principle of an alkaline fuel cell.*

Both electrodes, anode and cathode, are separated by a circulating electrolyte, a 6M potassium hydroxide solution (Fig.1). At the anode hydrogen reacts with hydroxyl ions into water and free electrons, Eq. (1):

$$H_2 + 2\,OH^- \rightarrow 2\,H_2O + 2\,e^- \qquad (1)$$

Within the electrolyte, the water is transported from the anode to the cathode. An external electric circuit leads the electrons to the cathode. At the cathode oxygen reacts with water and electrons into hydroxyl ions, Eq. (2):

$$\tfrac{1}{2}\,O_2 + H_2O + 2\,e^- \rightarrow \quad 2\,OH^- \qquad (2)$$

These ions ow from cathode to anode through the electrolyte, to sustain the total electrochemical reaction. Combining both reactions the overall reaction, Eq. (3), shows that the end product is water, which can be removed in one or both gas streams or in the electrolyte, depending on the fuel cell configuration.

$$H_2 + \tfrac{1}{2}\,O_2 \rightarrow \quad H_2O \qquad (3)$$

The overall reaction is exo-energetic. This energy has an electric part, which is transferred in the external electric circuit, and a thermal part, which results in a temperature rise inside the fuel cell. To maintain the overall fuel cell temperature, heat is removed by outlet mass flows or by losses to the environment.

Model assumptions

As discussed in [11] several models were already presented (See references in 11). Most of them focused on the electrical behaviour, one of them made assumptions on the mass balance. All previous models made assumptions on the water removal and suggested that it occurred in one of the gas streams. These assumptions were used as a boundary condition for the model.

In this work the water management will be a model result instead on a model input or boundary condition. Also the possibility of water disposal into the electrolyte, is included.

For the model a control volume approach is used. The model is divided into 5 areas (See Fig.2), each with their own physical and thermodynamic behaviour. For each control volume the mass and energy balance are posed. Next to this, the following assumptions were made:

- Dynamic pressure losses within the fuel cell are neglected. In this way the total pressure can be assumed constant over the entire fuel cell. The same approach is used for a PEM fuel cell in [12], which is more critical than AFC to pressure drops, because it has no liquid electrolyte.
- The temperature is assumed to be uniform in each control volume and all output flows have this temperature, which is similar to the approach in [11, 12].
- The partial pressures within the gas chambers are the mean (partial) pressures of the input and output flow in the direction of the gas.
- The heat losses from the gas chambers to the environment are neglected, because the heat transfer surface is relatively small. All heat losses to the environment are therefore modeled as heat losses of the fuel cell body to the environment.

The five parts which are considered in the control volume model, are the anode and cathode gas chambers (AGC and CGC), the anode and cathode gas diffusion layers (AGDF and CGDF) and the fuel cell body (FCB), where the reaction takes place (See Fig.2). The model is modularly built. In this way a more detailed model can be obtained by serially connecting several individual models. Table 1 gives an overview of the molar and energy flows shown in figure 2. New elements in this model, compared to earlier work [11] are:

- that the hydrogen and oxygen consumption and the water vapour removal of the fuel cell model is based upon diffusion laws. The diffusion is described by the Stefan-Maxwell equation, Eq.(4):

$$\frac{dy_i}{dz} = \frac{R.T}{P} \cdot \sum_j \frac{y_i.N_j - y_j.N_i}{D_{ij}} \quad (4)$$

- that the water vapour in the fuel cell body is assumed to be saturated. In this way a direct relation between cell temperature and partial pressure of water vapour can be posed, Eq.(5):

$$p = f(T) \quad (5)$$

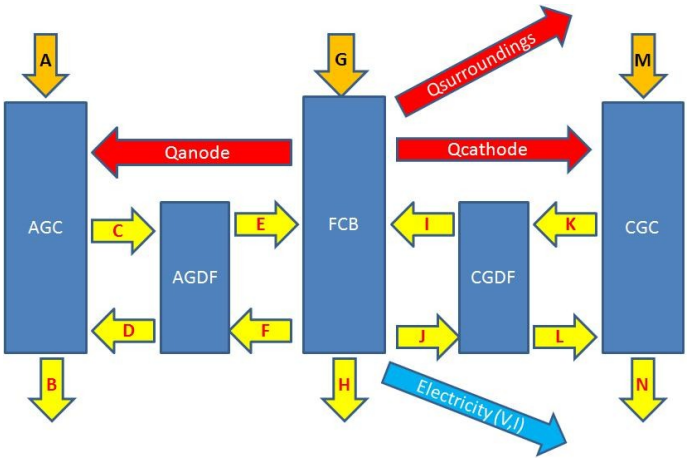

Figure 2 *Lay-out of the alkaline fuel cell model (See Table 1 for a detailed description).*

Model development

Anode gas chamber.

A mixture of hydrogen and water vapour (A) enters the gas chamber at certain temperature and pressure. Part of the hydrogen diffuses into the fuel cell (C), part of the formed water is removed by water vapour (D) in the hydrogen gas stream. A mixture of hydrogen and water vapour leaves the gas chamber (B) at normally a higher temperature and at same pressure.

The mass and energy balances are used to relate all variables to the input. In the mass balance it is taken into account that the system subject to our research is an end –of-pipe-system, which means no hydrogen leaves the last gas chamber (B).

In the energy balance the heat flux is considered to be convective and related to the gas speed [11].

The (partial) pressure of C and D are an weighted average of the partial pressures of hydrogen and water vapour in flows A and B.

Cathode gas chamber.

A similar approach is used for the cathode side, wet air (oxygen, nitrogen and water vapour) enters(M) and leaves the gas chamber (N). Next to an extra component, nitrogen, the cathode side isn't end-of-pipe. This will result in two extra degrees of freedom in the mass balance. The rest is similar to the anode.

Name	Description
AGC	Anode gas chamber, part of the hydrogen flow channel in contact with the fuel cell.
AGDF	Anode gas diffusion layer, boundary layer where gasses (hydrogen and water vapour) diffuse into and out of the fuel cell.
FCB	Fuel cell body, existing out of both catalytic layers (with the electrodes) and out of the separator layer (the electrolyte, in which the ion transport takes place.)
CGDF	Cathode gas diffusion layer, boundary layer where gasses (oxygen and water vapour) diffuse into and out of the fuel cell.
CGC	Cathode gas chamber, part of the air flow channel in contact with the fuel cell.
A	Input molar flow at the anode, containing hydrogen (and water vapour).
B	Output molar flow at the anode, containing water vapour (and hydrogen). \\
C	Molar flow of hydrogen, diffusing from AGC into FCB, at the boundary with AGC. \\
D	Molar flow of water vapour, diffusing from FCB into AGC, at the boundary with AGC. \\
E	Molar flow of hydrogen, diffusing from AGC into FCB, at the boundary with FCB. \\
F	Molar flow of water vapour, diffusing from FCB into AGC, at the boundary with FCB. \\
G	Input molar flow for FCB, containing electrolyte (water).
H	Output molar flow from FCB, containing electrolyte (water).
I	Molar flow of oxygen, diffusing from CGC into FCB, at the boundary with FCB.
J	Molar flow of water vapour, diffusing from FCB into CGC, at the boundary with FCB.
K	Molar flow of oxygen, diffusing from CGC into FCB, at the boundary with CGC.
L	Molar flow of water vapour, diffusing from FCB into CGC, at the boundary with CGC.
M	Input molar flow for CGC, containing (wet)air
N	Output molar flow from CGC, containing wet air
Q_{anode}	Energy flow: (convective) heat transfer from FCB to AGC.
$Q_{cathode}$	Energy flow: (convective) heat transfer from FCB to CGC.
$Q_{surroundings}$	Energy flow: heat losses to the environment.
Electricity	Energy flow: generated electricity.

Table 1 *Description of the control volumes and the molar and energy flows in Fig.2.*

Anode gas diffusion chamber

Between gas chamber and active surface a layer can be defined in which the diffusion or migration of the gases towards the reaction zone takes place. In absence of a global pressure drop between the gas chamber and fuel cell body, the driving force behind this migration is the concentration

difference of the gases between the gas chamber and the boundary of the fuel cell body.

This concentration difference is captured in the partial pressure difference between fuel cell body and gas chamber. The pressure of the intermediate flows (C,D,E,F) in the model are in fact partial pressures. For example pressure of C is the partial pressure of hydrogen in the anode gas chamber and pressure of E will be the partial pressure of hydrogen at the boundary with the fuel cell body. Taking this into account the Stefan-Maxwell equation (4) results in one independent differential equation, describing the diffusion and the lack of global pressure drop between the two boundaries (one of the assumptions, mentioned above).

$$\frac{dy_H}{dz} = \frac{R.T}{P} \cdot \frac{y_H.(N_w + N_H) - N_H}{D_{Hw}} \qquad (6)$$

As boundary condition the molar fraction in the gas chamber is set equal to a weighted mean of input and output flow, which was also the case for the (partial) pressure. Therefore at the anode side the molar fractions are in relation to the pressures of C and D. At the side of the fuel cell body (z= L_{GDF}) they are in relation to those of E and F.

Cathode gas diffusion chamber

A similar approach can be used at the cathode side, only this time the extra component, nitrogen, results in an extra coupled diffusion equation. This will result in a second degree differential equation for the molar fraction of oxygen. The boundary conditions are similar to those for the anode.

Fuel cell body

Next to the equations given in [11] equation (5) will be used to determine the boundary conditions for the diffusion at the side of the fuel cell body.

In the mass balance the law of Faraday relates hydrogen, oxygen, formed water and electric current to each other.

The energy balance does not only consist of molar flows and heat fluxes to other control volumes, but also to heat losses to the environment and electricity generation. The electrolyte flow (G and H) is modeled to be liquid water.

MODEL VALIDATION

The model is validated using experimental data which were generated with the AFC system described in detail in [**Fout! Verwijzingsbron niet gevonden.**, **Fout! Verwijzingsbron niet gevonden.**]. Part of these experimental results were discussed in [11]. Further data analysis is performed to evaluate the new element in the model, i.e. the water management.

Experimental set-up

Figure 3 shows a schematic view of the experimental set-up. Table 2 gives a brief description of the main operating parameters, marked on Fig.3.

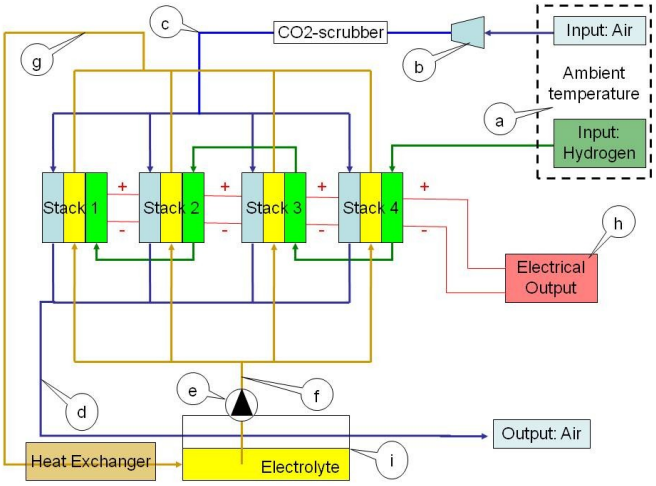

Figure 3 *Experimental set-up (description in Table 2)*

Parameter	Description	Measuring method
a	Ambient temperature (input temperature for air and hydrogen supply)	Direct
b	Air flow	Indirect
c	Air temperature	Estimated
d	Output air temperature	Direct
e	Electrolyte flow	Indirect
f	Input electrolyte temperature	Direct
g	Output electrolyte temperature	Direct
h	Total voltage, Current, cell voltages	Direct
i	Level of the electrolyte in the tank	Direct

Table 2 *List of operating parameter marked on Fig. 3*

For a detailed description of the parameters a to h in the experimental set-up we refer to earlier work, where the same experimental data were used to validate a previous model [11]. Next to the already discussed parameters the level of electrolyte is measured (point i). The measurement however is not that precise, because the water surface is not stable.

This is caused by the KOH-pump which switches between working steps and by the output air flow which passes over the electrolyte tank. Only an evaluation of the water level - with consideration of changes in electrolyte flow (point e) - over a long period of time will indicate when there is a net evaporation of water (electrolyte) or when there is a net formation of liquid water during this period of time.

Model validation

Current-which is directly proportional to the input hydrogen flow - input air flow rate, input electrolyte flow rate and input electrolyte temperature are used as input parameters for model

validation. The model is used to predict electrical performance, thermal behaviour and water management.
The model will be validated on these three aspects, which can be characterized by voltage, output temperatures for both electrolyte and air and by output flow rate of the liquid electrolyte. The validation is performed in two stages.

- First the model is compared with the previous model [11] and validated regarding the prediction on voltage and thermal behaviour, using a number of experimental data. The selection of these working points is described in [11].
- Secondly the water management is validated by selecting a long period in which the fuel cell is relatively stable and the electrolyte level is monitored.

Validation with existing experimental data
As described in ref. [11], all measured parameters are subject to instabilities. Data analysis led to a data set of 50 working points. The measured parameters, which are used as model input, are illustrated by a representative selection of data points. This selection is based on current and electrolyte temperature, the two most determining input parameters. The first two working points are representative for the range in which the data were obtained: the first one represents the lower bound and the second one the upper bound for both current and electrolyte temperature. The next four data points are all measured at the same average current, over a wide range of electrolyte temperatures. The last four are all measured at about the same average electrolyte temperature over a wide range of currents. The measured and modeled output parameters of these ten data points are shown in figures 4, 5 and 6.

In each of these figures the experimental data are compared to the model also ref. [11] and to this new model, described in this paper.

- The experimental output is represented by dots with error bars, which represent the instability on the measurement.
- The output of the model is represented by a floating bar. The line in the middle of this bar represents the modeled output of the mean input. The outer limits represent the measurement error on the input values.
- The results of the previous model in [11] is represented with a circle. For this model the measurement error on the input parameters was not taken into account.

In Figure 4 the prediction on electric performance is shown. The data is arranged by ascending current and electrolyte temperature, in case of similar currents (data points 7 to 10). The model shows a better performance on prediction of the voltage, compared to [11].

In Figures 5 and 6 the thermal behaviour is shown. Figure 5 shows the prediction of the output electrolyte temperature. The model has comparable results to [11], in predicting the electrolyte temperature.

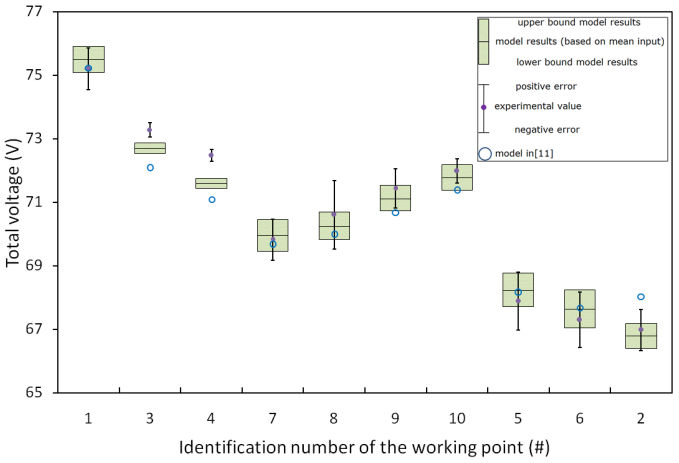

Figure 4 *Model verification on electric performance (voltage) with a number of working points arranged by ascending current and temperature in case of equal current (points 7 to 10). For every point the model prediction (floating bars) is compared to the experiments (dots) and the model in[11](circles).*

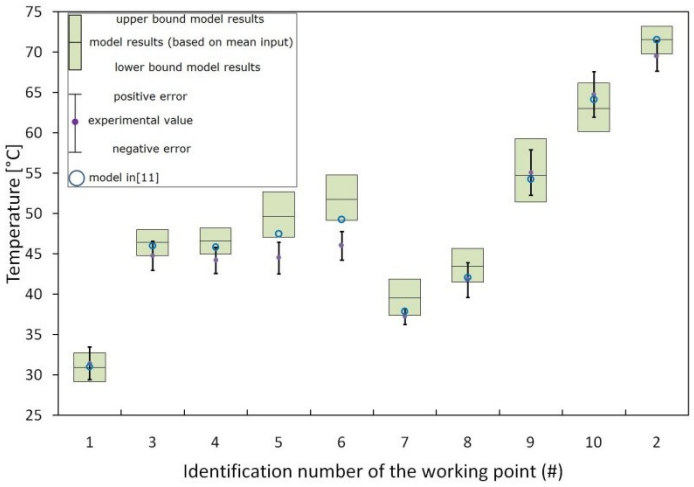

Figure 5 *Model verification, output electrolyte temperature. Data points 3 to 6 have all the same input electrolyte temperature and are arranged by ascending current. Data points 7 to 10 have all the same current and are arranged by ascending input electrolyte temperature. Data points 1 and 2 are the two most extreme values, considering current and input electrolyte temperature. For every point the model prediction (oating bars) is compared to the experiments (dots) and the model in[11](circles).*

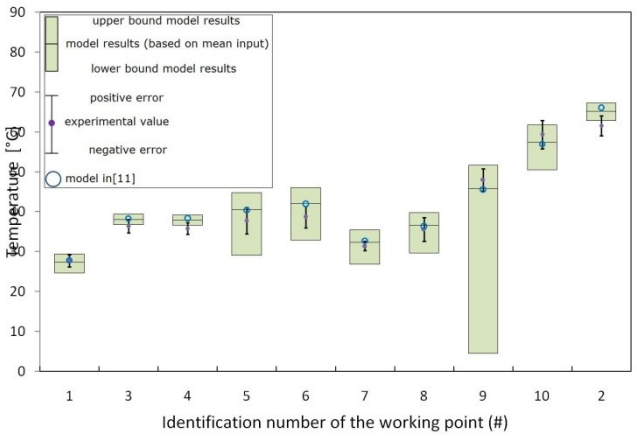

Figure 6 *Model verification, output air temperature. Data points 3 to 6 have all the same input electrolyte temperature and are arranged by ascending current. Data points 7 to 10 have all the same current and are arranged by ascending input electrolyte temperature. Data points 1 and 2 are the two most extreme values, considering current and input electrolyte temperature. For every point the model prediction (floating bars) is compared to the experiments (dots) and the model in [11](circles).*

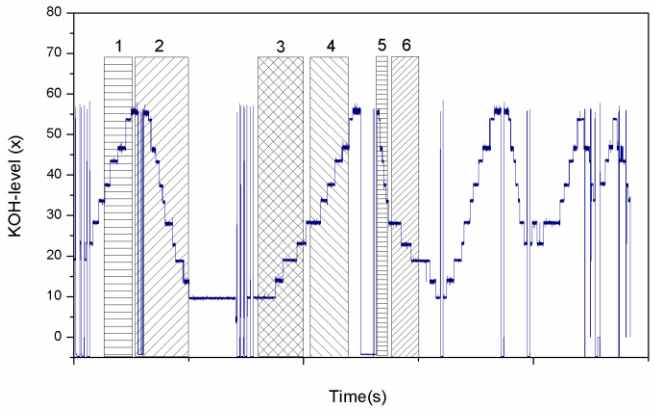

Figure 7 *Measured fluctuation of the electrolyte level in the KOH-tank during time of the experiments. Six periods are selected in which the input parameters are relatively stable and marked on the figure.*

Figure 6 shows the prediction of the output air temperature. For all 50 working points there is an overlap. Next to that, the relation with the electrolyte temperature is noticeable, both in the measurements as in the model. Therefore, the model is acceptable to predict thermal behaviour. Still the prediction of the air temperature is sensitive to the air flow, the parameter with the highest error range. As a result the modeled output shows a large difference between upper and lower boundary. The most remarkable result is the lower bound in working point 9. This represents an impossible situation, due to the high standard deviation in the measured air flow. The point however shows one of the limitations of the model, since it is assumed that the air flow is controlled to be at least sufficient to compensate the hydrogen input in Faraday's law. This assumption is not fulfilled in point 9, so the model cannot be used with those input conditions.

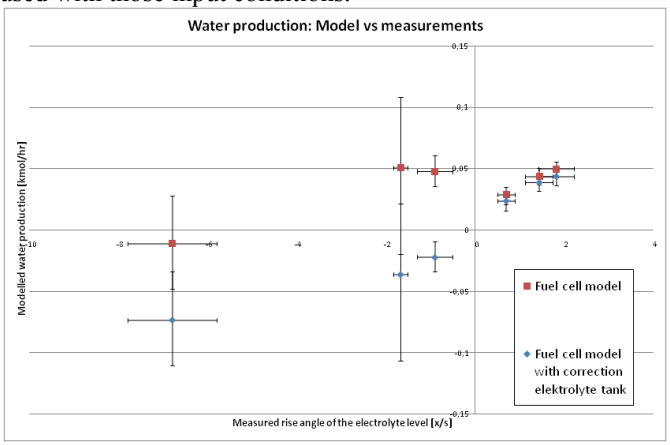

Figure 8 *Prediction of liquid water production vs measured rise of electrolyte level. Both for the fuel cell model (triangle) as for the extended model with the electrolyte tank (dots) the model results are set as a function of the measurements.*

Validation on the water management

To validate the model regarding the water management, the level of the electrolyte in the KOH-tank is monitored in time over the duration of the experiments (Fig.7). In this time period it was possible to determine 6 periods in which the electrolyte level shows a clear and steady change and in which the variation on the inlet conditions was relatively stable.

These conditions were used as input data for our model to predict the water production in the electrolyte flow, which will result a rise (or reduction) of the electrolyte level in the KOH-tank. If the model is representative to reflect the measurements, the modeled water production is directly proportional to the speed at which the measured electrolyte level rises.

In Figure 8 the model results for the formation of liquid water in the electrolyte flow (Y-axis) are set as a function of the measured rise per unit of time of the electrolyte level in the KOH-tank (X-axis). These data sets are represented by the triangles, which are expected to be in a straight line through the origin. However, when the electrolyte level drops the model overestimates the formation of liquid water in the electrolyte.

This could be due to the fact that the output air, which is not saturated, passes the tank. Assuming that this passage will result in an increased relative humidity (RH%) of the output air, more water will be evaporated at higher air flow rate and higher temperature, resulting in a lower electrolyte level.

To verify this the evaporation in the electrolyte tank is modeled as a function of electrolyte temperature, electrolyte flow rate, air flow rate, air temperature, relative humidity of air and percentage of evaporation: 0 means no evaporation - 100 means that the air is completely saturated.

Adding the evaporative effect of the KOH-tank to the model validation shows that the model predictions on the production of liquid water are confirmed by the experimental results (See figure 8). These are presented by the dots, which are aligned including the origin. This means that the model extension is sufficient and important to understand the results of the experimental set-up.

ANALYSIS OF THE WATER MANAGEMENT

With the validated model a sensitivity analysis is performed to gain insight in the effect of every input parameter on the water management within the fuel cell. For the analysis the influence of seven parameters is examined (See Table 3). The cumulated influence of the first two parameters, current and electrolyte temperature with any other parameter is examined at every new condition, determined by the other _ve parameters. Table 3 presents an overview of the different inputs that are analysed below.

Parameter	average	minimum	maximum	stepsize
Current	20A-80A	20A	80A	10A
Input KOH temp	30°C-75°C	30°C	75°C	15°C
Input air temp	20°C	5°C	65°C	15°C
Input air RV%	0%	0%	100%	50%
Input air flow (air ratio)	2,5	1	8	1,5
KOH flow	20,5 kmol/hr	19 kmol/hr	22 kmol/hr	1,5 kmol/hr
Temp surrounding	20°C	-10°C	50°C	15°C

Table 3 List examined parameters

Influence of the electrolyte

To evaluate the influence of the electrolyte, both electrolyte flow rate and electrolyte temperature at the input were set at different values.

The electrolyte flow shows no significant influence on the water management. The electrolyte temperature however has a large impact on the water management. In figure 9 is shown that at low electrolyte temperature almost no water vapour diffuses and that the formed liquid water is proportional to the current, which is directly linked to the generated water (See also figure 10).

The impact of the electrolyte temperature on the evaporation is proportional to its impact on the saturation pressure. At least a temperature of about 55 °C has to be reached to avoid net rise of liquid water in the electrolyte flow. At lower temperatures the saturation pressure drops rapidly. Because of this the driving force for the water vapour diffusion is strongly reduced. As a result liquid water builds up due to the formation of water, which is not transported out of the fuel cell by diffusion. For the same reason, but now in the opposite direction, there is a net evaporation at temperatures higher than 75_C, at least for currents within nominal working range (20A to 80A). To avoid dry out of the fuel cell, 75°C is to be set as a maximum temperature when working with dry or cold air. This will limit the electric efficiency since this is higher at higher temperature [11].

Influence of current

At low temperature current has no significant influence and all formed water will end up in the electrolyte flow. Figure 10 shows that for every input electrolyte temperature higher than the minimum value (about 55°C) a current can be found at which all formed water is evaporated and diffuses into the gas streams. This is interesting regarding steady state working points.

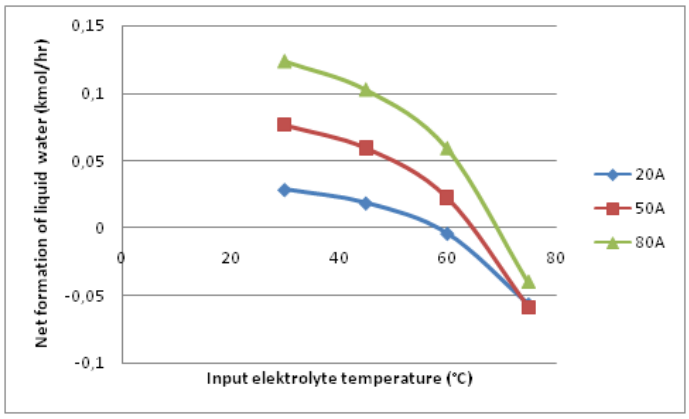

Figure 9*: Sensitivity of liquid water production to electrolyte temperature at three different currents.*

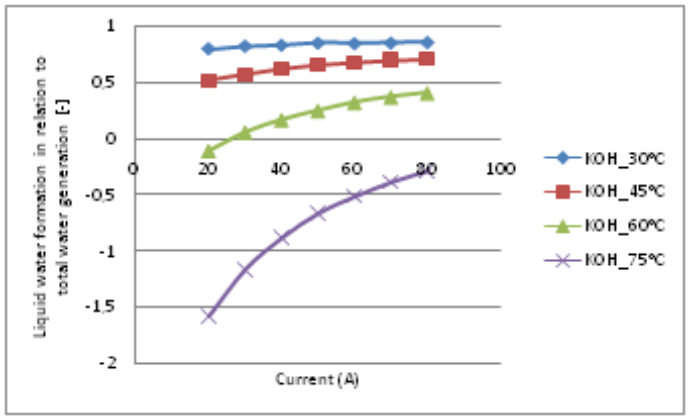

Figure 10: *Sensitivity of liquid water production to total current at four different electrolyte temperatures.*

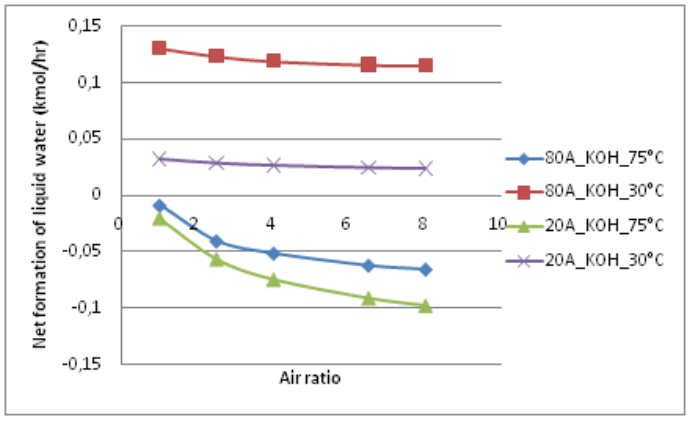

Figure 11 *Sensitivity of liquid water production to air ratio.*

Influence of the input air

To understand the influence of the air stream, three parameters were evaluated:

- the air ratio or the actual air flow rate in relation to the necessary air flow rate
- the relative humidity
- the air temperature

Figure 11 shows that a higher air ratio has a negative effect on the net formation of liquid water. The relative impact of an

increased air ratio reduces after a ratio of 2,5 to 4 (See Fig. 11). Naturally, the impact of the air ratio on the evaporation of the electrolyte tank is directly related, as shown in the model validation.

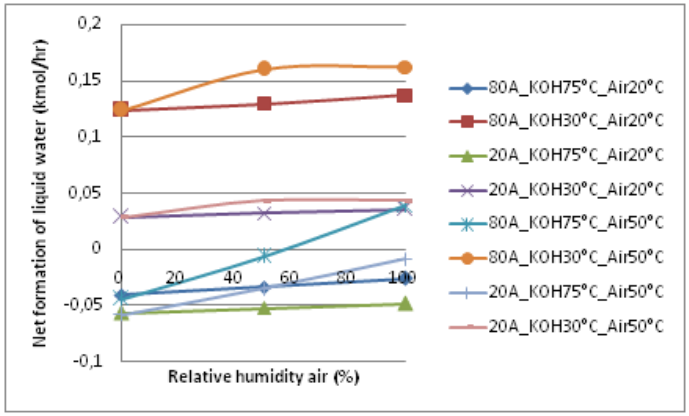

Figure 12 *Sensitivity of liquid water production to relative humidity and air temperature. For 8 different combinations of currents (20A or 80A), electrolyte temperature (30°C or 75°C) and air temperature (20°C or 50°C) the net formation of liquid water is set as a function of the relative humidity of the input air.*

Next to the air ratio, the temperature and relative humidity will be of importance. Their effect however, is relatively low. If the input air is dry, the air temperature has only a very small positive effect on the diffusion, which results in a lower net liquid water formation.

The relative humidity only has a large impact at high input air temperature (See Fig. 12). At lower temperature the water vapour content of saturated air is a lot lower and will have no significant influence on the water vapour content of the heated output air stream. To avoid dry out of the fuel cell a maximum temperature of the electrolyte has to be respected. However, this statement was posed using dry and cold air as inlet for the cathode. In Fig. 12 is shown that at higher electrolyte temperature it is still possible to maintain water content of the electrolyte flow, if hot humidified air is used as input for the fuel cell. Because electrolyte temperature has a positive effect on the fuel cell performance [11], this could increase the efficiency of the fuel cell.

CONCLUSION

A model of an alkaline fuel cell is created in Matlab. The model predicts the thermodynamic behaviour and water management of the fuel cell and is validated with experimental data from a system designed for CHP-applications. The influence of the input parameters on the water management is investigated.

- To maintain the concentrations within the electrolyte, a minimum electrolyte temperature has to be reached (about 55_C) to operate at low current.
- Higher currents will require higher input temperatures of the electrolyte to maintain the electrolyte concentration.
- The electrolyte temperature at a given current can be increased without dry out using hot humidified air.
- An air ratio higher than 2,5 is no more effective as a control paramater to maintain electrolyte concentration within the fuel cell.

REFERENCES

[1] M. Pehnt, Environmental impacts of distributed energy systems-The case of micro cogeneration, Environmental science and policy II (2008),25-37.
[2] M. De Paepe, P. D'Herdt, D. Mertens, Micro-CHP systems for residential applications, Energy Conversion and Management, Volume 47, Issues 18-19, November 2006,Pages 3435-3446.
[3] K. Alanne, A. Saari, Sustainable small-scale CHP technologies for buildings: the basis for multi-perspective decision-making, Renewable and Sustainable Energy Reviews,Volume 8, Issue 5 (October 2004) Pages 401-431.
[4] A.D. Hawkes, D.J.L. Brett, N.P. Brandon, Fuel cell micro-CHP techno-economics, International Journal of Hydrogen Energy 34(2009)9545-9557.
[5] I. Staffell, A. Ingram, Life cycle assessment of an alkaline fuel cell CHP system, International Journal of Hydrogen 35(2010) 2491-2505.
[6] H.I. Onovwiona, V.I. Ugursal, Residential cogeneration systems: review of the current technology, Renewable and Sustainable Energy reviews 10 (2006) 389-431.
[7] I. Staffell, A review of small stationary fuel cell performance , http : //wogone.com=iq=reviewofuelcellperformance:pdf(2009)[cited December 2010].
[8] G.F. Mclean,T. Niet,S. Prince-Richard,N. Djilali, An assessment of alkaline fuel cell technology, International Journal of Hydrogen Energy 275(2002)507-526.
[9] E. Gulzow, J.K. Nor, P.K. Nor and M. Schulze, A renaissance for alkaline fuel cells The fuel cell review, Volume 3 Issue 1 (2006).
[10] E. Gulzow,M. Schulze, U. Gerke, Bipolar concept for alkaline fuel cells International Journal of Power Sources 156(2006)1-7.
[11] I. Verhaert, M. De Paepe, G. Mulder, Thermodynamic Model for an Alkaline Fuel Cell, Journal of Power Sources 193(1) (2009); 193(1) 233-240.
[12] H.Huisseune, A. Willockx, M. De Paepe, Semiempirical along-the-channel model for a proton exchange membrane fuel cell International Journal of Hydrogen Energy, Volume 33, Issue 21 (November 2008)6270-6280.